Contrasting Behaviors of ^{210}Pb and ^{210}Po in the Productive Shelf Water Versus the Oligotrophic Water

Hojong Seo, DongJoo Joung[†] and Guebuem Kim*

Research Institute of Oceanography, School of Earth and Environmental Sciences, Seoul National University, Seoul, South Korea

We measured the total, truly dissolved (<10 kDa), colloidal (10 kDa–0.2 μm), and particulate phases (>0.2 μm) of ^{210}Pb and ^{210}Po in the East China Sea (ECS) shelf water and the East Sea (Japan Sea). In order to examine the behaviors of ^{210}Pb and ^{210}Po in different marine environments, we compiled our results with previously reported data in the same region and in the northwestern Pacific Ocean (NWPO). The proportions of the truly dissolved, colloidal, and particulate phases in the shelf water were 32, 27, and 41% for ^{210}Pb and 49, 32, and 19% for ^{210}Po, respectively. Based on a steady-state scavenging model, ^{210}Pb and ^{210}Po showed higher (3.0 ± 0.6 year^{-1}) and lower (0.3 ± 0.2 year^{-1}) scavenging rates, respectively, in the shelf water than those in the NWPO and the East Sea. A non-steady-state model, accounting for the residence time of the shelf water, also showed twice more efficient removal rate of ^{210}Pb in the shelf water than that in the NWPO and the East Sea. In contrast, there was the net input of ^{210}Po in the shelf water relative to the large removal in the NWPO and the East Sea. The large proportions of total dissolved (truly dissolved + colloidal) ^{210}Po (>80%) in the shelf water indicate active regeneration of ^{210}Po from the sinking particles and the surface sediments. Our results suggest that the ECS shelf is the source for Po in the northwestern Pacific marginal seas, a proxy for sulfur group elements (S, Se, and Te), whereas it is the efficient sink for Pb, together with other particle-reactive trace elements.

Keywords: ^{210}Pb, ^{210}Po, shelf water, scavenging, colloid

INTRODUCTION

Naturally occurring ^{210}Pb (half-life = 22.3 years) is produced from ^{222}Rn (half-life = 3.8 days), belonging to the ^{238}U decay series, and it produces ^{210}Po (half-life = 138.4 days). In oceanic environments, ^{210}Pb originates mainly from the atmospheric deposition in the upper ocean and *in situ* production from ^{226}Ra (half-life = 1,600 years) decay, *via* ^{222}Rn, in the deep ocean. Since the production of ^{210}Po from ^{210}Pb is negligible in the atmosphere, most ^{210}Po in the ocean is assumed to be produced from ^{210}Pb decay. Both ^{210}Pb and ^{210}Po are known to be particle reactive in aqueous systems, but ^{210}Po tends to be preferentially assimilated by marine biota (Fisher et al., 1983; Wei and Murray, 1994; Hung and Chung, 1998; Stewart and Fisher, 2003; Carvalho, 2011). This efficient biological removal of ^{210}Po results in disequilibria between ^{210}Pb and ^{210}Po in the upper ocean,

and this principle has been used to determine particulate organic carbon export (Bacon et al., 1976; Friedrich and van der Loeff, 2002; Stewart et al., 2007; Tang and Stewart, 2019).

Although the removal of ^{210}Po is known to be related to marine productivity, previous studies have reported a large deficiency of ^{210}Po in oligotrophic oceans (Nozaki et al., 1990a; Kim, 2001; Chung and Wu, 2005). Nozaki et al. (1990a) attributed such a distinct deficiency to the significant atmospheric input of ^{210}Pb. However, Kim (2001) suggested that an unusually large deficiency in the oligotrophic ocean could be due to the efficient uptake of ^{210}Po by cyanobacteria and then transfer to higher trophic levels along marine food chains rather than downward settling. On the contrary, in the eutrophic ocean, ^{210}Po may reside for a much longer time in the non-settling organic pool as it is taken up by free-living bacteria (Kim, 2001). This hypothesis was further supported by Chung and Wu (2005) in the South China Sea.

The East China Sea (ECS) shelf, including the Yellow Sea and the southern sea of Korea, is one of the largest continental shelves in the world. It has a total area of 3.6×10^5 km^2 with a mean depth of 70 m (Fang et al., 2009; Dong et al., 2011). This sea receives great amounts of nutrients from the Changjiang (e.g., 1.1×10^{11} mol year^{-1} for dissolved inorganic nitrogen; Dai et al., 2011) and also shows high primary productivity (510–580 mg C m^{-2} day^{-1}), which is 2.7 times higher than that in the adjacent Kuroshio water (Hama et al., 1997; Gong et al., 2000). As very oligotrophic Kuroshio water in the northwestern Pacific Ocean (NWPO) flows into the East Sea (Japan Sea) through this ECS shelf, significant biogeochemical alterations occur in the shelf water (Kim et al., 2018; Cho et al., 2019). The East Sea is a semi-enclosed marginal sea that has a total area of 1.0×10^6 km^2 with a maximum depth of over 3,500 m. This interconnected system (the NWPO–the ECS shelf water–the East Sea) may provide an ideal opportunity to study how chemical species behave in different biogeochemical conditions. However, only a few studies have examined the behaviors of ^{210}Pb and ^{210}Po according to the change in environmental conditions in this region. Thus, in this study, we aim to (1) investigate the behaviors of ^{210}Pb and ^{210}Po in different oceanic settings (productive shelf water versus oligotrophic water) and (2) understand the scavenging mechanisms of both radionuclides in association with colloids.

MATERIALS AND METHODS

Sampling

Sampling was conducted over two periods in the southern sea of Korea and the East Sea: from May 8 to 22, 2005, on the R/V *Tamgu* (Stn. C-1, C-2, C-3, and C-4), and from January 26 to February 2, 2018, on the R/V *ISABU* (Stn. S1, S4, E1, E5, and E8; **Figure 1**). Seawater samples for total ($\sim$10–20 L) and size fractionation ($\sim$40 L) were collected directly from Niskin bottles. To collect the size-fractionated samples, seawater was filtered through the 0.2-μm cartridge filter using a peristaltic pump. The pre-filtered (<0.2 μm) samples were separated into the truly dissolved (<10 kDa) and colloidal phases (10 kDa–0.2 μm) using a tangential flow filtration system (PLCGC, Pellicon, Millipore,

Burlington, MA, United States), which was pre-cleaned with 1 M HCl, 10 L deionized water, and 0.5 M NaOH (Guéguen et al., 2002; Baskaran et al., 2003; Kim and Kim, 2012, 2014). This filtration procedure was completed within 10 h after collection to avoid adsorption of particles onto the bottles. The filtered samples were acidified with 8 M nitric acid (pH $\sim$1) and transferred into 40-L plastic buckets.

^{210}Pb and ^{210}Po Analysis

The analytical methods for ^{210}Pb and ^{210}Po were adapted from Kim and Kim (2012). Briefly, the ^{209}Po spike (1 dpm), Pb^{2+} carrier (20 mg), and Fe^{3+} carrier (50 mg) were added to the seawater samples. After the equilibration, the pH was raised to 8 using NH$_4$OH to precipitate Fe(OH)$_3$, together with ^{210}Pb and ^{210}Po. The precipitates were allowed to settle for 4 h. After the supernatants were siphoned off, the precipitates were filtered using Whatman 41 grade paper. The precipitates and any organic matters in the sample were fully digested with the mixed solution of concentrated HNO$_3$, HCl, and HF and then converted to 0.5 M HCl. The samples were heated to 80°C after adding ascorbic acid (0.5 g) to reduce Fe^{3+} to Fe^{2+}. Po from the heated samples was simultaneously plated onto a silver disk while rotating the disk for 3 h using a magnetic stirrer. The ^{210}Po sources were counted using alpha spectrometry with a passivated implanted planar silicon detector (Alpha Analyst, Canberra, Australia). The remaining solution was further purified for ^{210}Pb analysis. Concentrated HNO$_3$ was added to the solution and heated to oxidize the ascorbic acid. After the solution was converted to 9 M HCl, it was loaded onto the pre-conditioned anion exchange column (AG 1 $\times$ 8 resin, Bio-Rad Laboratories, Hercules, CA, United States) to separate Pb. The eluents (Pb) were stored for more than 6 months for the ingrowth of ^{210}Po. The ^{210}Pb activity was determined *via* the ingrown ^{210}Po activity using the same Po plating and alpha counting procedures. The recovery of ^{210}Pb was obtained by measuring stable Pb in ^{210}Pb solutions using a magnetic sector field inductively coupled plasma mass spectrometer (ICP-MS; Element 2, Thermo Scientific, Waltham, MA, United States).

RESULTS

In order to examine the behaviors of ^{210}Pb and ^{210}Po in different oceanic settings, our results are compared with previously published data in the northwestern Pacific seas. The data are sorted into three regions: the NWPO (Tsunogai and Nozaki, 1971; Nozaki and Tsunogai, 1976; Nozaki et al., 1990a), the ECS shelf water (Lee et al., 1996; Hong et al., 1999; Su et al., 2017; this study), and the East Sea (Kim and Kim, 2012; this study; **Figure 1**). Data on the truly dissolved and colloidal phases of ^{210}Pb and ^{210}Po are only available in this study (ECS shelf water) and in Kim and Kim (2012; East Sea). Although the stations of Lee et al. (1996) and stations E1, S1, and S4 in this study are located in the southwestern part of the East Sea, they are included in the ECS shelf water data because they are located downstream of the ECS shelf water flows (Morimoto and Yanagi, 2001; Chang et al., 2004, 2016). Some data near the Changjiang (Hong et al., 1999;
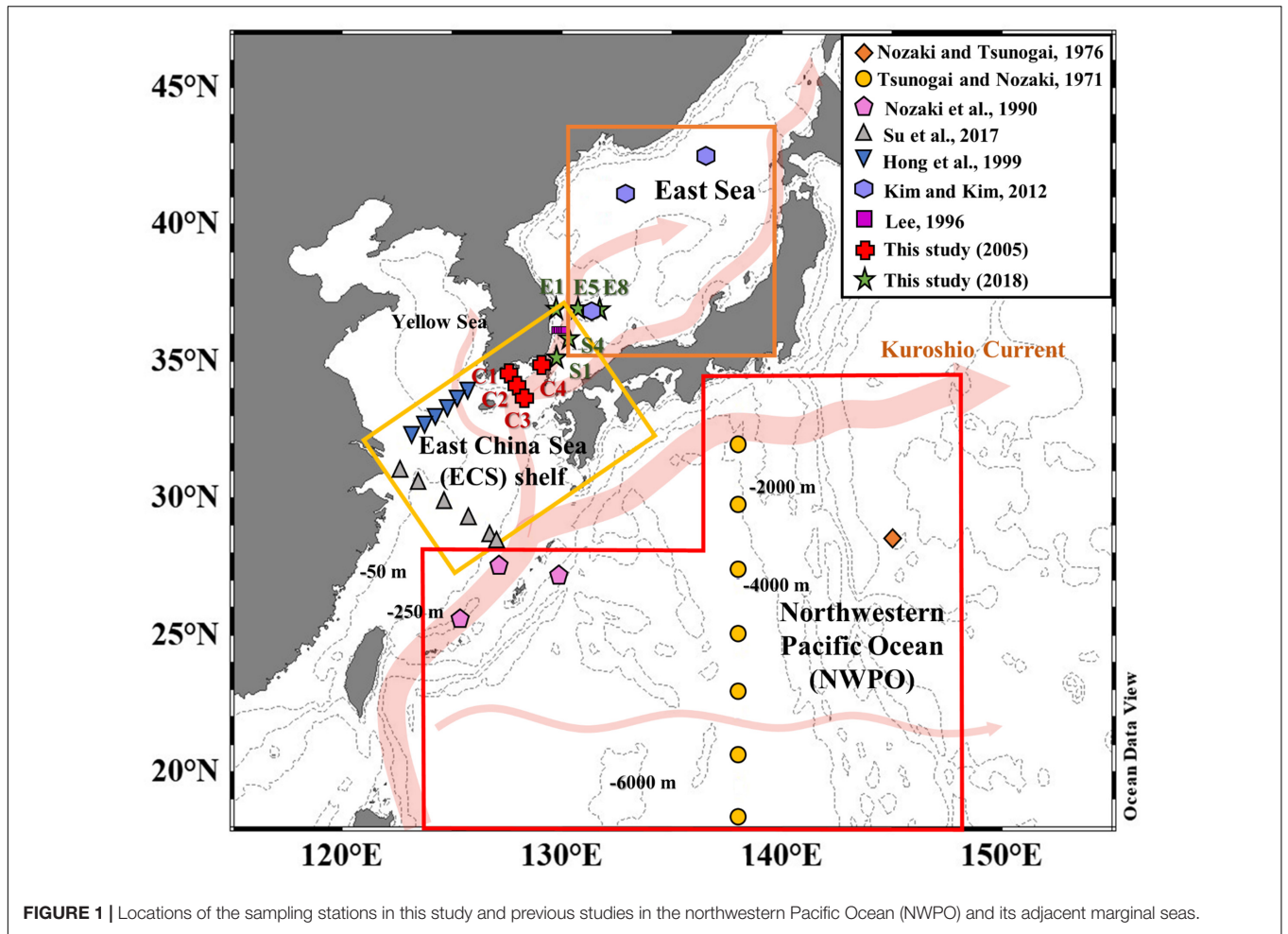
FIGURE 1 | Locations of the sampling stations in this study and previous studies in the northwestern Pacific Ocean (NWPO) and its adjacent marginal seas.
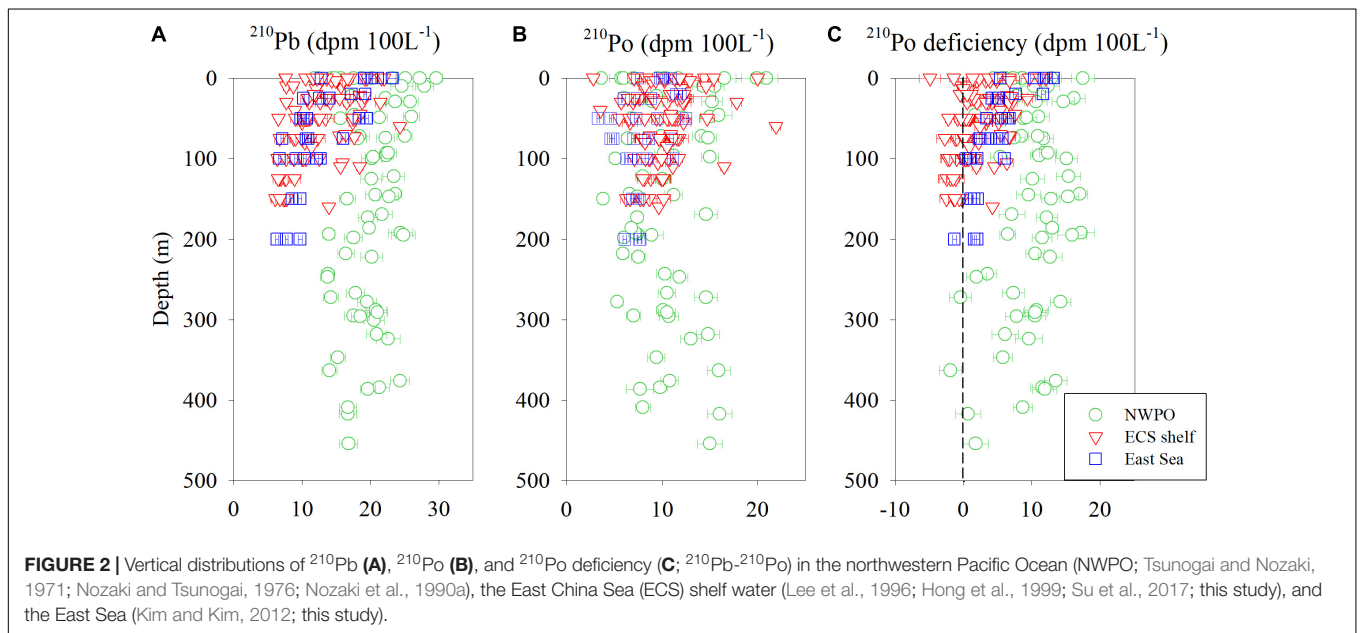
FIGURE 2 | Vertical distributions of ^{210}Pb **(A)**, ^{210}Po **(B)**, and ^{210}Po deficiency **(C)**; ^{210}Pb-^{210}Po) in the northwestern Pacific Ocean (NWPO; Tsunogai and Nozaki, 1971; Nozaki and Tsunogai, 1976; Nozaki et al., 1990a), the East China Sea (ECS) shelf water (Lee et al., 1996; Hong et al., 1999; Su et al., 2017; this study), and the East Sea (Kim and Kim, 2012; this study).

FIGURE 3 | Proportions of ^{210}Pb **(A)** and ^{210}Po **(B)** in truly dissolved (<10 kDa), colloidal (10 kDa–0.2 μm), and particulate (>0.2 μm) phases in the East China Sea (ECS) shelf water and the East Sea.
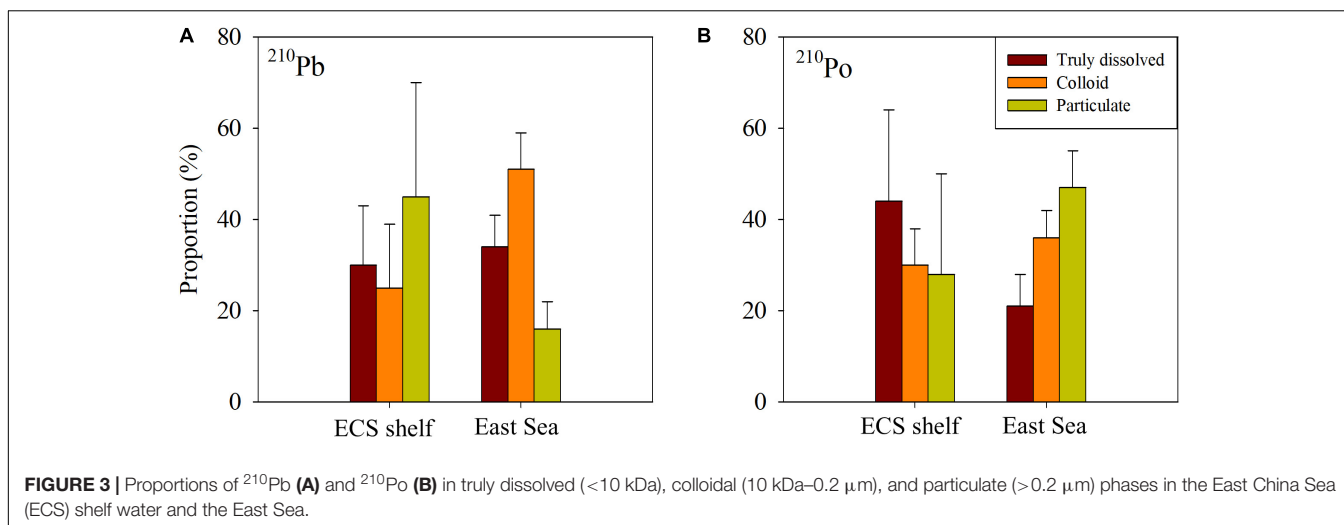
Su et al., 2017) and the southern Yellow Sea (Hong et al., 1999), which show unusually high activities (^{210}Po/^{210}Pb ratios > 1), are excluded since they are considered to be significantly influenced by terrestrial sources. All the analytical results of our experiments are given in **Supplementary Table 1**.

In the surface layer (0–25 m), the activities of total ^{210}Pb were lower in the ECS shelf water (14 ± 3 dpm 100 L^{-1}) relative to the NWPO (20 ± 6 dpm 100 L^{-1}) and the East Sea (17 ± 4 dpm 100 L^{-1}; **Figure 2A**). The distributions of total ^{210}Pb generally showed maximum values in the surface layer and decreased with depth in the three regions, as observed in other major oceans (e.g., Nozaki et al., 1980; Kim, 2001; Rigaud et al., 2015; Horowitz et al., 2020). For example, the activities of total ^{210}Pb decreased by approximately 50, 20, and 50% from 0 to 150 m in the ECS shelf water, the NWPO, and the East Sea, respectively. In the ECS shelf water, several stations showed maximum ^{210}Pb activities near the bottom sediments, which were 1.5–2.0 times higher than those in the surface layer. Of the total activities, the proportions of truly dissolved, colloidal, and particulate ^{210}Pb in the ECS shelf water were about 32 ± 13%, 27 ± 14%, and 41 ± 24%, whereas those in the East Sea were about 34 ± 7%, 51 ± 8%, and 16 ± 6%, respectively (**Figure 3A**). There was no significant difference in the activities of truly dissolved and colloidal phases between the ECS shelf water and the East Sea. However, the activities of particulate ^{210}Pb in the ECS shelf water were about four times higher than those in the East Sea (**Supplementary Table 1**).

For total ^{210}Po activities, there was no distinct difference in the surface layer (0–25 m) among the ECS shelf water (11 ± 3 dpm 100 L^{-1}), the NWPO (11 ± 5 dpm 100 L^{-1}), and the East Sea (10 ± 2 dpm 100 L^{-1}; **Figure 2B**). As such, there was no clear trend with depth. However, there was a significant difference in the deficiency of ^{210}Po (^{210}Pb-^{210}Po) in the three regions (**Figure 2C**). The most oligotrophic NWPO showed a relatively larger deficiency (9 ± 4 dpm 100 L^{-1}) in the upper ocean (0–25 m) compared with those in the East Sea (7 ± 3 dpm 100 L^{-1}) and the ECS shelf water (3 ± 3 dpm 100 L^{-1}). The largest deficiency of ^{210}Po in the NWPO was observed at 200 m, while it was observed in the surface layer and decreased with depth in

the ECS shelf water and the East Sea. Of the total activities, the proportions of truly dissolved, colloidal, and particulate ^{210}Po in the ECS shelf water were about 48 ± 19%, 31 ± 8%, and 24 ± 21%, whereas those in the East Sea were about 21 ± 7%, 36 ± 6%, and 47 ± 8%, respectively (**Figure 3B**). The activities of ^{210}Po in the ECS shelf water were approximately 3.8, 1.7, and 1.8 times higher than those in the East Sea for the truly dissolved, colloidal, and particulate phases, respectively (**Supplementary Table 1**).

DISCUSSION

Steady-State and Non-steady-State Scavenging Models for ^{210}Pb and ^{210}Po

A steady-state (SS) scavenging model is used to estimate the scavenging rates of ^{210}Pb and ^{210}Po in this study, as utilized by previous studies in open ocean (e.g., Bacon et al., 1976; Obata et al., 2004; Murray et al., 2005). At steady state ($\partial A/\partial t = 0$), if advection and diffusion are neglected, the scavenging rate constants of ^{210}Pb and ^{210}Po can be calculated using the following equations:

For ^{210}Pb:

$$\frac{\partial A_{Pb}^{t}}{\partial t} = \lambda_{Pb} \times \left(A_{Ra} - A_{Pb}^{t}\right) + F_{Atm} - A_{Pb}^{t} k_{Pb}^{t} = 0 \quad (1)$$

$$\frac{\partial A_{Pb}^{td}}{\partial t} = \lambda_{Pb} \times \left(A_{Ra} - A_{Pb}^{td}\right) + F_{Atm} - A_{Pb}^{td} k_{Pb}^{td} = 0 \quad (2)$$

$$\frac{\partial A_{Pb}^{c}}{\partial t} = \lambda_{Pb} \times \left(-A_{Pb}^{c}\right) + A_{Pb}^{td} k_{Pb}^{td} - A_{Pb}^{c} k_{Pb}^{c} = 0 \quad (3)$$

$$\frac{\partial A_{Pb}^{p}}{\partial t} = \lambda_{Pb} \times \left(-A_{Pb}^{p}\right) + A_{Pb}^{c} k_{Pb}^{c} - A_{Pb}^{p} k_{Pb}^{p} = 0 \quad (4)$$

For ^{210}Po:

$$\frac{\partial A_{Po}^{t}}{\partial t} = \lambda_{Po} \times \left(A_{Pb}^{t} - A_{Po}^{t}\right) - A_{Po}^{t} k_{Po}^{t} = 0 \quad (5)$$

$$\frac{\partial A_{Po}^{td}}{\partial t} = \lambda_{Po} \times \left(A_{Pb}^{td} - A_{Pb}^{td}\right) - A_{Po}^{td} k_{Po}^{td} = 0 \quad (6)$$

$$\frac{\partial A_{Po}^{c}}{\partial t} = \lambda_{Po} \times \left(A_{Pb}^{c} - A_{Pb}^{c}\right) + A_{Po}^{td} k_{Po}^{td} - A_{Po}^{c} k_{Po}^{c} = 0 \quad (7)$$

$$\frac{\partial A_{Po}^{p}}{\partial t} = \lambda_{Po} \times \left(A_{Pb}^{p} - A_{Pb}^{p}\right) + A_{Po}^{c} k_{Po}^{c} - A_{Po}^{p} k_{Po}^{p} = 0 \quad (8)$$

where λ, A, F_{Atm}, and k are the decay constant (day^{-1}), inventory of element (dpm m^{-2}), atmospheric depositional flux of ^{210}Pb (55 dpm m^{-2} day^{-1}; Nozaki et al., 1973; Turekian et al., 1977), and the scavenging rate constant (year^{-1}), respectively. t, td, c, and p represent the total, truly dissolved, colloidal, and particulate phases, respectively. To obtain the activities of ^{226}Ra in the ECS shelf water, the empirical relationship with salinity is used for the southern sea of Korea (Stn. C-1, C-2, C-3, and C-4; Yang et al., 1992, 1996), and the data from Wang et al. (2018c) are used for the other ECS shelf regions. The activities of ^{226}Ra in the NWPO and the East Sea are from previously published results (Nozaki and Tsunogai, 1976; Chung and Craig, 1980; Harada and Tsunogai, 1986; Nozaki et al., 1990b). The riverine inputs are neglected because ^{210}Pb is almost completely trapped in the Changjiang estuary (Wang et al., 2018b). The atmospheric input of ^{210}Po is also neglected since the ^{210}Po/^{210}Pb ratios in precipitation in this study region are lower than 0.2 (Kim et al., 2005a; Yan et al., 2012).

The hydrological conditions and biogeochemical processes in the ECS shelf water are significantly affected by the intrusion of the NWPO (Wang et al., 2018a; Zuo et al., 2019; Liu et al., 2021). The chemical properties of the intruded water undergo rapid changes during the water residence times in the ECS shelf. Therefore, the removal fluxes of ^{210}Pb and ^{210}Po in the ECS shelf water can be calculated using the non-steady-state (NSS) model, accounting for the residence times of the shelf water. The removal fluxes of ^{210}Pb and ^{210}Po in the ECS shelf water are expressed by the following equations:

$$\frac{\partial A_{Pb}^{ECS}}{\partial t} = \lambda_{Pb} \times \left(A_{Ra}^{ECS} - A_{Pb}^{ECS}\right) + F_{Atm} - R_{Pb}^{ECS} + F_{lateral, Pb} \quad (9)$$
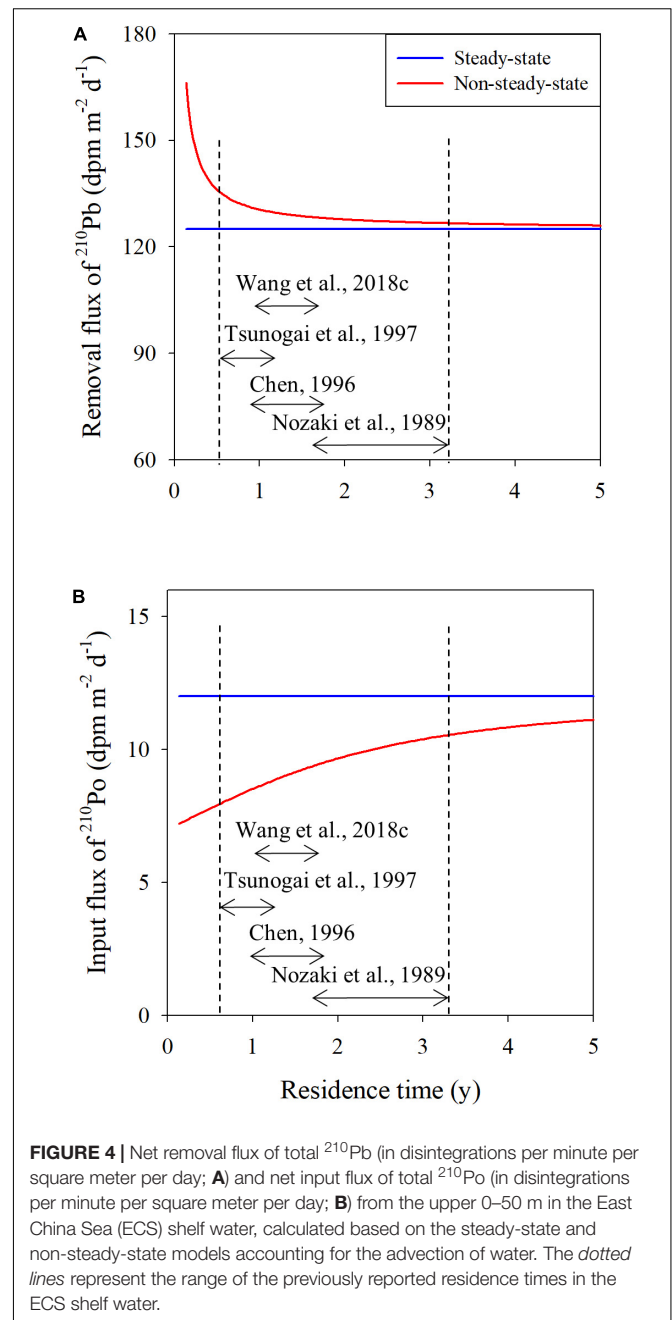
$$\frac{\partial A_{Po}^{ECS}}{\partial t} = \lambda_{Po} \times \left(A_{Pb}^{ECS} - A_{Po}^{ECS}\right) - R_{Po}^{ECS} + F_{lateral, Po} \quad (10)$$

where R and $F_{lateral}$ are the removal flux (in disintegrations per minute per square meter per day) and the lateral transport of the radionuclide by current, respectively. Assuming that A_{Ra}, F_{Atm}, R, and $F_{lateral}$ are constant during a given time interval, the solutions for Eqs 9, 10 are expressed as follows (based on the work by Friedrich and van der Loeff, 2002):

$$R_{Pb}^{ECS} = F_{atm} + F_{lateral, Pb} + \lambda_{Pb} A_{Ra}^{ECS} +$$

$$\frac{\lambda_{Pb}}{1 - e^{-\lambda_{Pb}\Delta t}}\left(A_{Pb,t1} e^{-\lambda_{Pb}\Delta t} - A_{Pb,t2}\right) \quad (11)$$

$$R_{Po}^{ECS} = F_{lateral, Po} + \frac{\lambda_{Po}}{1-e^{-\lambda_{Po}\Delta t}}\left[\frac{\lambda_{Pb} A_{Ra}^{ECS} + F_{atm} + F_{lateral, Pb} - R_{Pb}^{ECS}}{\lambda_{Pb}}\right.$$

$$\left\{\frac{\lambda_{Po}}{\lambda_{Po}-\lambda_{Pb}}\left(e^{-\lambda_{Po}\Delta t} - e^{-\lambda_{Pb}\Delta t}\right) + \left(1-e^{-\lambda_{Po}\Delta t}\right)\right\}$$

$$\left. + A_{Pb,t1}\frac{\lambda_{Po}}{\lambda_{Po}-\lambda_{Pb}}\left(e^{-\lambda_{Pb}\Delta t} - e^{-\lambda_{Po}\Delta t}\right) + A_{Po,t1}e^{-\lambda_{Po}\Delta t} - A_{Po,t2}\right]$$

$$(12)$$

In this calculation, we assume that the water of the NWPO enters the ECS shelf at time t_1 and stays for an amount of time Δt (t_2-t_1). Therefore, Δt is the residence time of the ECS shelf water. A_{t1}

FIGURE 4 | Net removal flux of total ^{210}Pb (in disintegrations per minute per square meter per day; **A**) and net input flux of total ^{210}Po (in disintegrations per minute per square meter per day; **B**) from the upper 0–50 m in the East China Sea (ECS) shelf water, calculated based on the steady-state and non-steady-state models accounting for the advection of water. The *dotted lines* represent the range of the previously reported residence times in the ECS shelf water.

and A_{t2} are the activities of radionuclides in the NWPO and the ECS shelf water, respectively. The lateral transport term ($F_{lateral}$) is calculated by multiplying the current velocity of ~20 cm s^{-1} (Ichikawa and Beardsley, 2002; Lee et al., 2014) by the activity gradient between the NWPO and the ECS shelf water along the 400-km distance (Yangtze River mouth–Jeju Island). The calculated results using Eqs 11, 12 according to the change in residence times of the ECS shelf water are shown in **Figure 4**. The SS model, which accounts for the advection of water, is given for comparison.

Behaviors of ^{210}Pb and ^{210}Po

The scavenging rate constant of total ^{210}Pb in the ECS shelf water (3.0 ± 0.6 year^{-1}) was relatively higher than that in the NWPO (2.2 ± 0.4 year^{-1}) and the East Sea (2.6 ± 0.4 year^{-1}) based on the SS model (**Table 1**). The corresponding values of truly dissolved and colloidal ^{210}Pb in the ECS shelf water were also 1.2–2.0 times higher than those in the East Sea. However, the scavenging rate constant of particulate ^{210}Pb in the ECS shelf water was approximately 3.8 times lower than that in the East Sea, perhaps associated with the higher activities of particulate ^{210}Pb in the ECS shelf water. Given that the maximum activities of particulate ^{210}Pb were observed in the surface layer at C3 and the

bottom layer at C4, respectively, such high activities of particulate ^{210}Pb might be attributed to the lateral input from land or the resuspension from the bottom sediments. This could occur due to the shallow water depth and by episodic storm events (Choi et al., 2004, 2010). In both cases, the SS model is not appropriate for calculating the scavenging rate constant and removal flux in the ECS shelf water.
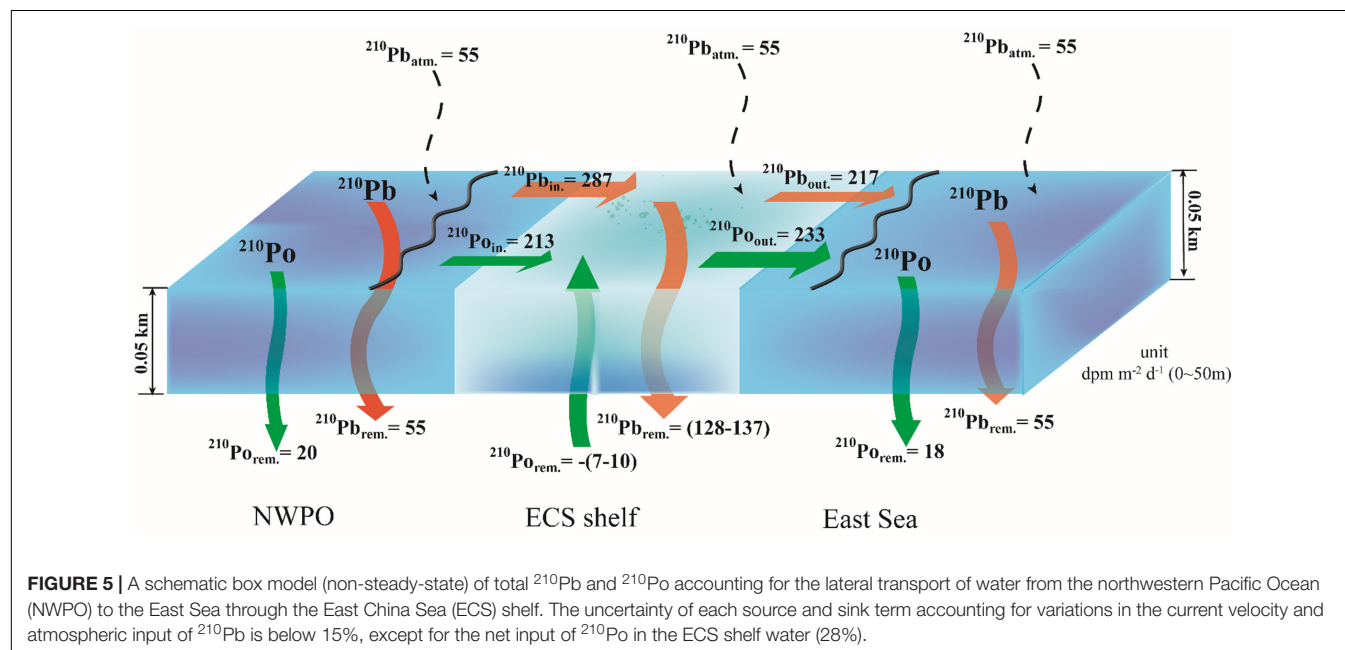
Based on the NSS model, total ^{210}Pb was more effectively removed in the ECS shelf water (128–137 dpm m^{-2} day^{-1}) relative to the NWPO (55 dpm m^{-2} day^{-1}) and the East Sea (55 dpm m^{-2} day^{-1}; **Figure 5**). The removal flux of total ^{210}Pb showed differences from 1 to 9% between the NSS and SS models within the previously reported residence times of the ECS shelf water (0.5–3.1 years; **Figure 4A**; Nozaki et al., 1989; Chen, 1996; Tsunogai et al., 1997; Wang et al., 2018c). These high scavenging rate and removal flux of ^{210}Pb in the ECS shelf water might be due to the higher concentrations of the suspended particulate matters in the ECS shelf water (6.8–15.0 mg L^{-1}; Bi et al., 2020) compared with those in the NWPO (0.1–0.3 mg L^{-1}; Hung and Chan, 1998) and the East Sea (0.2–0.6 mg L^{-1}; Chen et al., 1996; Hong et al., 2008).

For ^{210}Po, the scavenging rate constant of total ^{210}Po in the ECS shelf water (0.3 ± 0.2 year^{-1}) was much lower than that in

TABLE 1 | Scavenging rate constants (per year) of total, truly dissolved (<10 kDa), colloidal (10 kDa–0.2 μm), and particulate (>0.2 μm) ^{210}Pb and ^{210}Po in the upper 0–50 m of the northwestern Pacific Ocean (NWPO), the East China Sea (ECS) shelf water, and the East Sea.

Location	Total		Truly dissolved (<10 kDa)		Colloidal (10 kDa–0.2 or 0.45 μm)		Particulate (>0.2 or 0.45 μm)	
	^{210}Pb	^{210}Po	^{210}Pb	^{210}Po	^{210}Pb	^{210}Po	^{210}Pb	^{210}Po
NWPO	2.2 ± 0.4	1.3 ± 0.5	–	–	–	–	–	–
ECS shelf water	3.0 ± 0.6	0.3 ± 0.2	8.6 ± 0.3	0.2[a]	11.3 ± 1.7	0.3[a]	6.1 ± 0.2	4.5 ± 3
East Sea	2.6 ± 0.4	1.8 ± 0.3	7.4 ± 1.1	5.9 ± 3.2	5.8 ± 1.3	6.5 ± 2.1	23.6 ± 7.6	3.8 ± 1.1

[a]The C4 station showed a negative scavenging constant due to the equilibrium state between ^{210}Pb and ^{210}Po.

FIGURE 5 | A schematic box model (non-steady-state) of total ^{210}Pb and ^{210}Po accounting for the lateral transport of water from the northwestern Pacific Ocean (NWPO) to the East Sea through the East China Sea (ECS) shelf. The uncertainty of each source and sink term accounting for variations in the current velocity and atmospheric input of ^{210}Pb is below 15%, except for the net input of ^{210}Po in the ECS shelf water (28%).

the NWPO (1.3 ± 0.5 year^{-1}) and the East Sea (1.8 ± 0.3 year^{-1}), which is opposite to the ^{210}Pb trend (**Table 1**). Especially, the truly dissolved and colloidal ^{210}Po in the ECS shelf water approached equilibrium with ^{210}Pb. The calculated results of the NSS model showed the net input of ^{210}Po in the ECS shelf water (7–10 dpm m^{-2} day^{-1}), opposite to the net removal in the NWPO (20 dpm m^{-2} day^{-1}) and the East Sea (18 dpm m^{-2} day^{-1}; **Figure 5**). The net input flux of ^{210}Po increased with the residence times of the ECS shelf water and showed a difference from 13 to 35% between the NSS and SS models (**Figure 4B**).

These distinctively low scavenging rate constant and net input flux of ^{210}Po have been reported in the ECS (Nozaki et al., 1991), Gulf of Lion (Radakovitch et al., 1998), and northwestern Mediterranean Sea (Masqué et al., 2002). Nozaki et al. (1991) and Radakovitch et al. (1998) argued that this trend might be due to the extensive inputs of suspended particulate matters from river discharges with ^{210}Po/^{210}Pb ratios of ∼1. On the other hand, Masqué et al. (2002) suggested that the incorporation of ^{210}Po into the organic matter following the uptake by buoyant particles resulted in the low scavenging rate constant of ^{210}Po. In this study, we discount the riverine sources as the main reason for the low scavenging rate constant of ^{210}Po because the influence of river discharge with high ^{210}Po/^{210}Pb ratios was excluded in the comparison. In addition, the ^{210}Po/^{210}Pb ratios were ∼0.5 for the particulate phase and ∼1 for the total dissolved (truly dissolved + colloidal) phases in the ECS shelf water.

In general, low contents of organic carbon (0.2–1.0%) were observed in the sinking particles and the bottom sediments in the ECS shelf, associated with rapid organic carbon remineralization (Lin et al., 2000, 2002; Iseki et al., 2003). The results of sediment core incubation also showed that the organic carbon remineralization rate in the bottom sediments accounted for 12–24% of the primary productivity in this highly eutrophic ECS shelf water (Song et al., 2016), indicating the efficient regeneration of organic matter in the bottom sediments. In addition, hypoxia occurred intermittently in the bottom of ECS shelf water (dissolved oxygen concentrations <2–3 mg L^{-1}; Chen et al., 2007), which can also increase the net input flux of ^{210}Po as insoluble Po(IV) can be reduced to soluble Po(II) (Balistrieri et al., 1995; Kim et al., 2005b; Kim and Kim, 2014). Considering the relatively higher proportions of the total dissolved (truly dissolved + colloidal) ^{210}Po in the ECS shelf water (>80%), the colloidal matter might be associated with the net input of ^{210}Po due to regeneration from the sinking particles and in the bottom sediments.

Thus, our results suggest that ^{210}Po, a proxy for sulfur group elements (S, Se, and Te), may reside longer in the water column because of active regeneration, while ^{210}Pb and other particle-reactive elements would be removed in association with the large population of the sinking particles in the shelf water.

CONCLUSION

The scavenging rate constant and removal flux of ^{210}Pb and ^{210}Po were estimated using a geochemical scavenging model

in the productive shelf system connected to the oligotrophic NWPO. The scavenging rate constant of ^{210}Pb was relatively higher (3.0 ± 0.6 year^{-1}) in the ECS shelf water, whereas that of ^{210}Po was lower (0.3 ± 0.2 year^{-1}) than that in the NWPO and the East Sea. In addition, a NSS model accounting for the ocean currents showed the effective removal of ^{210}Pb in the ECS shelf water (128–137 dpm m^{-2} day^{-1}), whereas ^{210}Po showed the net input from the sinking particles and the bottom sediments (7–10 dpm m^{-2} day^{-1}). Given that the largest proportions of ^{210}Pb and ^{210}Po were particulate and total dissolved (truly dissolved + colloidal) phases, respectively, these opposite behaviors could be due to the efficient scavenging of ^{210}Pb versus the efficient regeneration of ^{210}Po from organic matter in the ECS shelf water. Thus, our results suggest that particle-reactive elements would be effectively removed in the shelf water, whereas sulfur group elements (S, Se, and Te) might be supplied from the sinking particles and the bottom sediments by efficient regeneration.

DATA AVAILABILITY STATEMENT

The original contributions presented in the study are included in the article/**Supplementary Material**, further inquiries can be directed to the corresponding author/s.

AUTHOR CONTRIBUTIONS

GK contributed to the conceptualization of the study. HS and DJ performed field sampling and analyses. HS and GK were involved in the data interpretation and writing of the manuscript. All authors contributed to the final version of the manuscript.

FUNDING

ACKNOWLEDGMENTS

SUPPLEMENTARY MATERIAL

The Supplementary Material for this article can be found online at: https://www.frontiersin.org/articles/10.3389/fmars.2021.701441/full#supplementary-material

REFERENCES

Bacon, M., Spencer, D., and Brewer, P. (1976). ^{210}Pb/^{226}Ra and ^{210}Po/^{210}Pb disequilibria in seawater and suspended particulate matter. *Earth Planet. Sci. Lett.* 32, 277–296.

Balistrieri, L. S., Murray, J. W., and Paul, B. (1995). The geochemical cycling of stable Pb, ^{210}Pb, and ^{210}Po in seasonally anoxic Lake Sammamish, Washington, USA. *Geochim. Cosmochim. Acta* 59, 4845–4861. doi: 10.1016/0016-7037(95)00334-7

Baskaran, M., Swarzenski, P., and Porcelli, D. (2003). Role of colloidal material in the removal of ^{234}Th in the Canada basin of the Arctic Ocean. *Deep Sea Res. 1 Oceanogr. Res. Pap.* 50, 1353–1373. doi: 10.1016/s0967-0637(03)00140-7

Bi, Q., Zhang, F., Deng, B., and Du, J. (2020). SPM control on the partitioning and balance of ^{210}Po and ^{210}Pb in high-turbidity surface waters of the East China Sea. *J. Environ. Radioact.* 222:106367. doi: 10.1016/j.jenvrad.2020.106367

Carvalho, F. P. (2011). Polonium (^{210}Po) and lead (^{210}Pb) in marine organisms and their transfer in marine food chains. *J. Environ. Radioact.* 102, 462–472. doi: 10.1016/j.jenvrad.2010.10.011

Chang, K.-I., Teague, W., Lyu, S., Perkins, H., Lee, D.-K., Watts, D., et al. (2004). Circulation and currents in the southwestern East/Japan Sea: overview and review. *Prog. Oceanogr.* 61, 105–156. doi: 10.1016/j.pocean.2004.06.005

Chang, K.-I., Zhang, C.-I., Park, C., Kang, D.-J., Ju, S.-J., Lee, S.-H., et al. (2016). *Oceanography of the East Sea (Japan Sea)*. Berlin: Springer.

Chen, C. (1996). The Kuroshio intermediate water is the major source of nutrients on the East China Sea continental shelf. *Oceanol. Acta* 19, 523–527.

Chen, C.-C., Gong, G.-C., and Shiah, F.-K. (2007). Hypoxia in the east China sea: one of the largest coastal low-oxygen areas in the world. *Mar. Environ. Res.* 64, 399–408. doi: 10.1016/j.marenvres.2007.01.007

Chen, C.-T. A., Lin, C.-M., Huang, B.-T., and Chang, L.-F. (1996). Stoichiometry of carbon, hydrogen, nitrogen, sulfur and oxygen in the particulate matter of the western North Pacific marginal seas. *Mar. Chem.* 54, 179–190. doi: 10.1016/0304-4203(96)00021-7

Cho, H. M., Kim, G., Kwon, E. Y., and Han, Y. (2019). Radium tracing cross-shelf fluxes of nutrients in the northwest Pacific Ocean. *Geophys. Res. Lett.* 46, 11321–11328. doi: 10.1029/2019gl084594

Choi, J.-Y., Kim, S.-Y., and Kang, H.-J. (2004). Distribution of suspended particulate matters in the east China sea, southern yellow sea and south sea of Korea during the winter season. *J. Korea Soc. Oceanogr.* 39, 212–221.

Choi, K.-H., Lee, S.-M., Lim, S.-M., Walton, M., and Park, G.-S. (2010). Benthic habitat quality change as measured by macroinfauna community in a tidal flat on the west coast of Korea. *J. Oceanogr.* 66, 307–317. doi: 10.1007/s10872-010-0027-7

Chung, Y., and Craig, H. (1980). ^{226}Ra in the Pacific Ocean. *Earth Planet. Sci. Lett.* 49, 267–292.

Chung, Y., and Wu, T. (2005). Large ^{210}Po deficiency in the northern South China sea. *Cont. Shelf Res.* 25, 1209–1224. doi: 10.1016/j.csr.2004.12.016

Dai, Z., Du, J., Zhang, X., Su, N., and Li, J. (2011). Variation of riverine material loads and environmental consequences on the Changjiang (Yangtze) Estuary in recent decades (1955- 2008). *Environ. Sci. Technol.* 45, 223–227. doi: 10.1021/es103026a

Dong, L., Guan, W., Chen, Q., Li, X., Liu, X., and Zeng, X. (2011). Sediment transport in the Yellow Sea and East China Sea. *Estuar. Coast. Shelf Sci.* 93, 248–258. doi: 10.1016/j.ecss.2011.04.003

Fang, T.-H., Li, J.-Y., Feng, H.-M., and Chen, H.-Y. (2009). Distribution and contamination of trace metals in surface sediments of the East China Sea. *Mar. Environ. Res.* 68, 178–187. doi: 10.1016/j.marenvres.2009.06.005

Fisher, N. S., Burns, K. A., Cherry, R., and Heyraud, M. (1983). Accumulation and cellular distribution of ^{241}Am, ^{210}Po, and ^{210}Pb in two marine algae. *Mar. Ecol. Prog. Ser.* 11, 233–237. doi: 10.3354/meps011233

Friedrich, J., and van der Loeff, M. M. R. (2002). A two-tracer (^{210}Po–^{234}Th) approach to distinguish organic carbon and biogenic silica export flux in the Antarctic circumpolar current. *Deep Sea Res. 1 Oceanogr. Res. Pap.* 49, 101–120. doi: 10.1016/s0967-0637(01)00045-0

Gong, G.-C., Shiah, F.-K., Liu, K.-K., Wen, Y.-H., and Liang, M.-H. (2000). Spatial and temporal variation of chlorophyll a, primary productivity and chemical hydrography in the southern East China Sea. *Cont. Shelf Res.* 20, 411–436. doi: 10.1016/s0278-4343(99)00079-5

Guéguen, C., Belin, C., and Dominik, J. (2002). Organic colloid separation in contrasting aquatic environments with tangential flow filtration. *Water Res.* 36, 1677–1684. doi: 10.1016/s0043-1354(01)00374-8

Hama, T., Shin, K., and Handa, N. (1997). Spatial variability in the primary productivity in the East China Sea and its adjacent waters. *J. Oceanogr.* 53, 41–51. doi: 10.1007/bf02700748

Harada, K., and Tsunogai, S. (1986). ^{226}Ra in the Japan Sea and the residence time of the Japan Sea water. *Earth Planet. Sci. Lett.* 77, 236–244. doi: 10.1016/0012-821x(86)90164-0

Hong, G.-H., Kim, Y.-I., Baskaran, M., Kim, S.-H., and Chung, C.-S. (2008). Distribution of ^{210}Po and export of organic carbon from the euphotic zone in the southwestern East Sea (Sea of Japan). *J. Oceanogr.* 64, 277–292. doi: 10.1007/s10872-008-0022-4

Hong, G.-H., Park, S.-K., Baskaran, M., Kim, S.-H., Chung, C.-S., and Lee, S.-H. (1999). Lead-210 and polonium-210 in the winter well-mixed turbid waters in the mouth of the Yellow Sea. *Cont. Shelf Res.* 19, 1049–1064. doi: 10.1016/s0278-4343(99)00011-4

Horowitz, E. J., Cochran, J. K., Bacon, M. P., and Hirschberg, D. J. (2020). ^{210}Po and ^{210}Pb distributions during a phytoplankton bloom in the North Atlantic: implications for POC export. *Deep Sea Res. I. Oceanogr. Res. Pap.* 164:103339. doi: 10.1016/j.dsr.2020.103339

Hung, G. W., and Chung, Y.-C. (1998). Particulate fluxes, ^{210}Pb and ^{210}Po measured from sediment trap samples in a canyon off northeastern Taiwan. *Cont. Shelf Res.* 18, 1475–1491. doi: 10.1016/s0278-4343(98)00032-6

Hung, J.-J., and Chan, C.-L. (1998). Distribution and enrichment of particulate trace metals in the southern East China Sea. *Geochem. J.* 32, 189–203. doi: 10.2343/geochemj.32.189

Ichikawa, H., and Beardsley, R. C. (2002). The current system in the Yellow and East China Seas. *J. Oceanogr.* 58, 77–92.

Iseki, K., Okamura, K., and Kiyomoto, Y. (2003). Seasonality and composition of downward particulate fluxes at the continental shelf and Okinawa Trough in the East China Sea. *Deep Sea Res. 2 Top. Stud. Oceanogr.* 50, 457–473. doi: 10.1016/s0967-0645(02)00468-x

Kim, G. (2001). Large deficiency of polonium in the oligotrophic ocean's interior. *Earth Planet. Sci. Lett.* 192, 15–21. doi: 10.1016/s0012-821x(01)00431-9

Kim, G., Hong, Y.-L., Jang, J., Lee, I., Hwang, D.-W., and Yang, H.-S. (2005a). Evidence for anthropogenic ^{210}Po in the urban atmosphere of Seoul, Korea. *Environ. Sci. Technol.* 39, 1519–1522. doi: 10.1021/es049023u

Kim, G., Kim, S.-J., Harada, K., Schultz, M. K., and Burnett, W. C. (2005b). Enrichment of excess ^{210}Po in anoxic ponds. *Environ. Sci. Technol.* 39, 4894–4899. doi: 10.1021/es0482334

Kim, J., Cho, H.-M., and Kim, G. (2018). Significant production of humic fluorescent dissolved organic matter in the continental shelf waters of the northwestern Pacific Ocean. *Sci. Rep.* 8:4887.

Kim, T.-H., and Kim, G. (2012). Important role of colloids in the cycling of ^{210}Po and ^{210}Pb in the ocean: results from the East/Japan Sea. *Geochim. Cosmochim. Acta* 95, 134–142. doi: 10.1016/j.gca.2012.07.029

Kim, T.-H., and Kim, G. (2014). Estimating benthic fluxes of trace elements to hypoxic coastal waters using ^{210}Po. *Estuar. Coast. Shelf Sci.* 151, 324–330. doi: 10.1016/j.ecss.2014.05.008

Lee, H., Kim, G., Kim, J., Park, G., and Song, K. H. (2014). Tracing the flow rate and mixing ratio of the Changjiang diluted water in the northwestern Pacific marginal seas using radium isotopes. *Geophys. Res. Lett.* 41, 4637–4645. doi: 10.1002/2014gl060230

Lee, H.-P., Yang, H.-S., and Kim, K.-H. (1996). Removal of ^{210}Po and ^{234}Th from seawater at the East-southern Coastal Region of Korea Peninsula in spring. *Bull. Korean Fish. Soc.* 29, 332–344.

Lin, S., Hsieh, I.-J., Huang, K.-M., and Wang, C.-H. (2002). Influence of the Yangtze River and grain size on the spatial variations of heavy metals and organic carbon in the east China Sea continental shelf sediments. *Chem. Geol.* 182, 377–394. doi: 10.1016/s0009-2541(01)00331-x

Lin, S., Huang, K.-M., and Chen, S.-K. (2000). Organic carbon deposition and its control on iron sulfide formation of the southern East China sea continental shelf sediments. *Cont. Shelf Res.* 20, 619–635. doi: 10.1016/s0278-4343(99)00088-6

Liu, Z., Gan, J., Hu, J., Wu, H., Cai, Z., and Deng, Y. (2021). Progress of studies on circulation dynamics in the east China sea: the kuroshio exchanges with the shelf currents. *Front. Mar. Sci.* 8:620910. doi: 10.3389/fmars.2021.620910

Masqué, P., Sanchez-Cabeza, J., Bruach, J., Palacios, E., and Canals, M. (2002). Balance and residence times of ^{210}Pb and ^{210}Po in surface waters of the northwestern Mediterranean Sea. *Cont. Shelf Res.* 22, 2127–2146. doi: 10.1016/s0278-4343(02)00074-2

Morimoto, A., and Yanagi, T. (2001). Variability of sea surface circulation in the Japan Sea. *J. Oceanogr.* 57, 1–13.

Murray, J. W., Paul, B., Dunne, J. P., and Chapin, T. (2005). ^{234}Th, ^{210}Pb, ^{210}Po and stable Pb in the central equatorial Pacific: tracers for particle cycling. *Deep Sea Res. 1 Oceanogr. Res. Pap.* 52, 2109–2139. doi: 10.1016/j.dsr.2005.06.016

Nozaki, Y., Ikuta, N., and Yashima, M. (1990a). Unusually large ^{210}Po deficiencies relative to ^{210}Pb in the Kuroshio Current of the East China and Philippine Seas. *J. Geophys. Res. Oceans* 95, 5321–5329. doi: 10.1029/jc095ic04p05321

Nozaki, Y., Kasemsupaya, V., and Tsubota, H. (1989). Mean residence time of the shelf water in the East China and the Yellow Seas determined by ^{228}Ra/^{226}Ra measurements. *Geophys. Res. Lett.* 16, 1297–1300. doi: 10.1029/gl016i011p01297

Nozaki, Y., Kasemsupaya, V., and Tsubota, H. (1990b). The distribution of ^{228}Ra and ^{226}Ra in the surface waters of the northern North Pacific. *Geochem. J.* 24, 1–6.

Nozaki, Y., Tsubota, H., Kasemsupaya, V., Yashima, M., and Naoko, I. (1991). Residence times of surface water and particle-reactive ^{210}Pb and ^{210}Po in the East China and Yellow seas. *Geochim. Cosmochim. Acta* 55, 1265–1272. doi: 10.1016/0016-7037(91)90305-o

Nozaki, Y., and Tsunogai, S. (1976). ^{226}Ra, ^{210}Pb and ^{210}Po disequilibria in the western North Pacific. *Earth Planet. Sci. Lett.* 32, 313–321.

Nozaki, Y., Tsunogai, S., and Nishimura, M. (1973). Lead-210 in the Japan Sea. *J. Oceanogr.* 29, 251–256. doi: 10.1007/bf02108844

Nozaki, Y., Turekian, K., and Von Damm, K. (1980). ^{210}Pb in GEOSECS water profiles from the North Pacific. *Earth Planet. Sci. Lett.* 49, 393–400. doi: 10.1016/0012-821x(80)90081-3

Obata, H., Nozaki, Y., Alibo, D. S., and Yamamoto, Y. (2004). Dissolved Al, In, and Ce in the eastern Indian Ocean and the Southeast Asian seas in comparison with the radionuclides ^{210}Pb and ^{210}Po. *Geochim. Cosmochim. Acta* 68, 1035–1048. doi: 10.1016/j.gca.2003.07.021

Radakovitch, O., Cherry, R. D., Heyraud, M., and Heussner, S. (1998). Unusual ^{210}Po/^{210}Pb ratios in the surface water of the Gulf of Lions. *Oceanol. Acta* 21, 459–468. doi: 10.1016/s0399-1784(98)80030-3

Rigaud, S., Stewart, G., Baskaran, M., Marsan, D., and Church, T. (2015). ^{210}Po and ^{210}Pb distribution, dissolved-particulate exchange rates, and particulate export along the North Atlantic US GEOTRACES GA03 section. *Deep Sea Res. 2 Top. Stud. Oceanogr.* 116, 60–78. doi: 10.1016/j.dsr2.2014.11.003

Song, G., Liu, S., Zhu, Z., Zhai, W., Zhu, C., and Zhang, J. (2016). Sediment oxygen consumption and benthic organic carbon mineralization on the continental shelves of the East China sea and the Yellow sea. *Deep Sea Res. 2 Top. Stud. Oceanogr.* 124, 53–63. doi: 10.1016/j.dsr2.2015.04.012

Stewart, G., Cochran, J., Miquel, J., Masqué, P., Szlosek, J., Rodriguez y Baena, A. M., et al. (2007). Comparing POC export from ^{234}Th/^{238}U and ^{210}Po/^{210}Pb disequilibria with estimates from sediment traps in the northwest Mediterranean. *Deep Sea Res. 1 Oceanogr. Res. Pap.* 54, 1549–1570. doi: 10.1016/j.dsr.2007.06.005

Stewart, G. M., and Fisher, N. S. (2003). Bioaccumulation of polonium-210 in marine copepods. *Limnol. Oceanogr.* 48, 2011–2019. doi: 10.4319/lo.2003.48.5.2011

Su, K., Du, J., Baskaran, M., and Zhang, J. (2017). ^{210}Po and ^{210}Pb disequilibrium at the PN section in the East China Sea. *J. Environ. Radioact.* 174, 54–65. doi: 10.1016/j.jenvrad.2016.07.031

Tang, Y., and Stewart, G. (2019). The ^{210}Po/^{210}Pb method to calculate particle export: lessons learned from the results of three GEOTRACES transects. *Mar. Chem.* 217:103692. doi: 10.1016/j.marchem.2019.103692

Tsunogai, S., and Nozaki, Y. (1971). Lead-210 and polonium-210 in the surface water of the Pacific. *Geochem. J.* 5, 165–173. doi: 10.2343/geochemj.5.165

Tsunogai, S., Watanabe, S., Nakamura, J., Ono, T., and Sato, T. (1997). A preliminary study of carbon system in the East China sea. *J. Oceanogr.* 53, 9–17. doi: 10.1007/bf02700744

Turekian, K. K., Nozaki, Y., and Benninger, L. K. (1977). Geochemistry of atmospheric radon and radon products. *Annu. Rev. Earth Planet. Sci.* 5, 227–255. doi: 10.1146/annurev.ea.05.050177.001303

Wang, C., Zou, X., Feng, Z., Hao, Z., and Gao, J. (2018a). Distribution and transport of heavy metals in estuarine–inner shelf regions of the East China sea. *Sci. Total Environ.* 644, 298–305. doi: 10.1016/j.scitotenv.2018.06.383

Wang, J., Zhang, W., Baskaran, M., Du, J., Zhou, F., and Wu, H. (2018b). Fingerprinting sediment transport in river-dominated margins using combined mineral magnetic and radionuclide methods. *J. Geophys. Res. Oceans* 123, 5360–5374. doi: 10.1029/2018jc014174

Wang, X., Baskaran, M., Su, K., and Du, J. (2018c). The important role of submarine groundwater discharge (SGD) to derive nutrient fluxes into river dominated ocean margins–the East China sea. *Mar. Chem.* 204, 121–132. doi: 10.1016/j.marchem.2018.05.010

Wei, C.-L., and Murray, J. W. (1994). The behavior of scavenged isotopes in marine anoxic environments: ^{210}Pb and ^{210}Po in the water column of the Black sea. *Geochim. Cosmochim. Acta* 58, 1795–1811. doi: 10.1016/0016-7037(94)90537-1

Yan, G., Cho, H.-M., Lee, I., and Kim, G. (2012). Significant emissions of ^{210}Po by coal burning into the urban atmosphere of Seoul. *Korea. Atmos. Environ.* 54, 80–85. doi: 10.1016/j.atmosenv.2012.02.090

Yang, H.-S., Kim, S.-S., and Lee, J.-C. (1996). Distribution characteristics of ^{210}Po and ^{210}Pb in the seawater from the Korean East sea in spring. *Bull. Korean Fish. Soc.* 29, 238–245.

Yang, H.-S., Kwon, Y.-A., Kim, G.-B., and Kim, S.-S. (1992). Distributions of ^{226}Ra and ^{228}Ra in the surface Waters of East sea of Korea. *Bull. Korean Fish. Soc.* 25, 399–405.

Zuo, J., Song, J., Yuan, H., Li, X., Li, N., and Duan, L. (2019). Impact of Kuroshio on the dissolved oxygen in the East China sea region. *J. Oceanol. Limnol.* 37, 513–524. doi: 10.1007/s00343-019-7389-5